Applied Soft Computing 110 (2021) 107721

Contents lists available at ScienceDirect

Applied Soft Computing

journal homepage: www.elsevier.com/locate/asoc

Conflict resolution in the multi-stakeholder stepped spillway design under uncertainty by machine learning techniques

Mehrdad Ghorbani Mooselu [a], Mohammad Reza Nikoo [b,*], Parnian Hashempour Bakhtiari [c], Nooshin Bakhtiari Rayani [d], Azizallah Izady [e]

[a] Department of Engineering Sciences, University of Agder, Norway
[b] Department of Civil and Architectural Engineering, Sultan Qaboos University, Muscat, Oman
[c] Department of Civil and Environmental Engineering, Shiraz University, Shiraz, Iran
[d] School of Engineering, Department of Civil and Environmental Engineering, Shiraz University, Shiraz, Iran
[e] Water Research Center, Sultan Qaboos University, Muscat, Oman

ARTICLE INFO

Article history:
Received 17 December 2020
Received in revised form 3 July 2021
Accepted 13 July 2021
Available online 22 July 2021

Keywords:
Stepped spillway
FLOW-3D®
CVaR-based optimization model
GMCR-plus
NSGA-II

ABSTRACT

The optimal spillway design is of great significance since these structures can reduce erosion downstream of the dams. This study proposes a risk-based optimization framework for a stepped spillway to achieve an economical design scenario with the minimum loss in hydraulic performance. Accordingly, the stepped spillway was simulated in the FLOW-3D® model, and the validated model was repeatedly performed for various geometric states. The results were used to form a Multilayer Perceptron artificial neural network (MLP-ANN) surrogate model. Then, a risk-based optimization model was formed by coupling the MLP-ANN and NSGA-II. The concept of conditional value at risk (CVaR) was utilized to reduce the risk of the designed spillway malfunctions in high flood flow rates, while minimizing the construction cost and the loss in hydraulic performance. Lastly, given the conflicting objectives of stakeholders, the non-cooperative graph model for conflict resolution (GMCR) was applied to achieve a compromise on the Pareto optimal solutions. Applicability of the suggested approach in the Jarreh Dam, Iran, resulted in a practical design scenario, which simultaneously minimizes the loss in hydraulic performance and the project cost and satisfies the priorities of decision-makers.

1. Introduction

Stepped spillways prevent erosion and consequently decrease the stilling basins' dimensions downstream of the dams [1,2]. The geometry of the stepped spillway (e.g., length and height of the spillway and steps' number) should be designed to maximize the hydraulic performance of the spillway (i.e., decreasing the probability of cavitation and increasing the energy dissipation). Flood flow uncertainty is of significant importance in the design and management of spillways and may pose serious risks to the hydraulic performance of the structure [3]. Flood flow estimation is complicated due to various factors such as roughness heterogeneity and variation in river geomorphology [4,5]. Yet, there is a lack of information on the effect of flood flow on the hydraulic performance of the spillway structure. Since existing designs are likely to experience losses in hydraulic performance, the present study seeks to address this issue by a risk-based optimization framework and achieve an economical design scenario with the minimum loss in hydraulic performance.

The optimal design of hydraulic structures is a multi-objective problem, including various conflicting objectives [3]. Convincing hydraulic performance is the primary concern in the design of stepped spillways. In this regard, various approaches have been applied, including physical and experimental models [6–11], numerical modeling [3,12–16], and data-driven or machine learning approaches [2,3,17,18]. Numerical simulation models such as Computational Fluid Dynamics (CFD) codes provided a proper context to evaluate the parameters, which were not explored/measured in physical models [12]. Further, soft computing methods were utilized to understand the non-linear relationships between design parameters and optimize the hydraulic properties [3,10,15,18,19].

Including the flood flow uncertainty in the design process, diverse classical optimization approaches such as linear programming [20,21], dynamic programming [22], and fuzzy optimization [3,23,24] have been applied to evaluate the risk of flood flow in the hydraulic structures' design. With the aim of overcoming the shortcomings of previous studies, the Conditional Value at Risk (CVaR) as a risk-based approach was applied in this study. CVaR is a novel approach for risk assessment, which has been efficiently utilized in a limited number of water-related topics such as water resources management studies [25–28].

* Corresponding author.
E-mail address: nikoo@squ.edu.om (M.R. Nikoo).

https://doi.org/10.1016/j.asoc.2021.107721
1568-4946/

Abbreviations

MLP-ANN	Multi-Layer Perceptron artificial neural network
NSGA-II	Nondominated Sorting Genetic Algorithm-II
VaR	Value-at-risk
CVaR	Conditional value at risk
GMCR	Graph model for conflict resolution
CFD	Computational Fluid Dynamics
KWPA	Khuzestan Water and Wastewater Company
ESM	Electronic Supplementary Material
VOF	Volume of Fluid
RNG	Renormalized Group
LES	Large Eddy Simulation
MARE	Mean Absolute Relative Error
SSE	Sum of Squared Errors
MSE	Mean Squared Error
GMR	General metarationality
SMR	Symmetric metarationality
SEQ	Sequential stability

Moreover, in a real case situation, the construction cost, which is the major objective of the project owner, is also a principal objective. Hence, the suggested scenarios should be determined considering the conflicts over the efficient design of the stepped spillway. Graph model for conflict resolution (GMCR) is a non-cooperative game model extensively used to analyze the conflict between decision-makers and provide a compromise strategy to resolve the conflicts [29,30]. The application of this model in the spillways' design has not been previously explored. Hence, in this study, the latest version, i.e., GMCR-plus, is applied in a real case problem.

The main aim of the present study is optimizing the stepped spillway design to achieve an economical design scenario with the minimum loss in hydraulic performance considering the flood flow uncertainty and conflicts between decision-makers. Therefore, the developed risk-based optimization model in this study attempts to minimize the risk of poor hydraulic performance while minimizing the construction cost (concrete volume) in the spillways' design process. To avoid inconsistencies and conflicting strategies between decision-makers, a GMCR model was also utilized, which considered the priority of the project owner and the designer in determining the final design scenario (compromise solution) among Pareto optimal solutions.

The proposed methodology included a three-dimensional FLOW-3D® model for flow simulation, the Multi-Layer Perceptron artificial neural network (MLP-ANN) surrogate model, a risk-based optimization framework using Non-dominated Sorting Genetic Algorithm II (NSGA-II), and a GMCR-plus model for addressing conflicts between decision-makers. The meta-heuristic methods were used in this study to investigate the risk of flood flow uncertainty in the hydraulic performance of the stepped spillways and consider the social complexities (priorities of decision-makers) in the design process. Also, the information of a physical model and numerical simulations were utilized to improve the suggested framework. The main contribution of this study is in the following cases, which have not been adequately attended in previous assessments:

(1) Developing a risk-based optimization model for spillway design relying on the results of a reduced-scale physical model and numerical simulations (developing FLOW-3D® model).

(2) Minimizing construction cost and the loss in hydraulic performance of stepped spillway by the concept of conditional value at risk.

(3) Conflict resolution in the design of stepped spillway considering the priorities of decision-makers by a developed GMCR-plus model.

The proposed methodology was evaluated in the Jarreh Dam, southern Iran. The results of the present study provide valuable knowledge on multi-objective optimization and conflict resolution in hydraulic structures' design.

2. Literature review

A literature review on the optimization of the spillway design demonstrates that previous studies have mostly focused on optimizing the spillway geometry considering the energy dissipation, cavitation index, and construction cost. Different meta-heuristic optimization algorithms (e.g., Genetic Algorithm, Gravitational Search Algorithm, Particle Swarm Optimization, and Artificial Bee Colony [31], Harris hawks optimization, particle swarm optimization, ANN-GA [32], NSGA-II [3,33], Differential Evolution (DE) algorithm [34], regression model [35]; shuffled frog leaping algorithm [36], Harmony Search Algorithm [37], gray wolf optimization [38], the honey-bee mating optimization [39,40]) have been successfully applied in this field, showing the efficiency of such algorithms in spillways design. Also, previous studies have proved the direct effect of uncertainties of the selected parameters on the obtained results [41,42]. The uncertainty caused by climate change [36,43] and flood flow [3,44,45] are known as the main uncertainties that has been considered in the optimal design of the spillway. Abrishamchi et al. 2003, integrated the uncertainty of flood magnitude and flood routing process in optimal design of spillway. They used fuzzy reasoning for the estimation of loss function [45]. The fuzzy method was also applied by Mooselu et al. 2019 to consider the flood flow uncertainty in optimal stepped spillway design [3]. The uncertainty of flood magnitude was considered in optimizing a spillway capacity by log Pearson Type III and Three-Parameter Lognormal Distribution functions [44]. However, considering flood uncertainty in stepped spillway design using a risk-based multi-objective optimization algorithm has not been considered yet. A risk-based optimization framework provides a proper context to include uncertainties in the decision-making process and improve design reliability [46]. In optimal risk-based design, the geometry/capacity of the hydraulic structure is determined to achieve the least risk value in total annual expected cost or loss in hydraulic performance [47]. The efficiency of the risk-based design has been explored in various hydraulic structures such as bridge design [48], flood levees [47], highway drainage structures [49], and flood diversion systems [46,50,51]. In this study, for the first time, we applied CVaR-NSGAII to minimize the loss in hydraulic performance and the construction cost of the stepped spillway. The proposed approach in this study is also useful in the decision-making process, especially when the decision-makers face economic, hydraulic, and hydrological uncertainties [46].

Furthermore, the application of the decision-making models for resolving the social complexities (conflicts) in the design of spillways is rare [3]. Hassanvand et al. 2019 applied a decision-making model (TOPSIS) for selecting the best type of spillway considering costs, time, and performance [37]. Mooselu et al. 2019 applied two decision-making models to achieve the lower and upper bounds of geometry in different confidence levels related to flood flow uncertainty in the optimal design of the stepped spillway [3]. Despite the importance of decision-makers priorities in the design process, the social complexities in spillway design have not been involved in spillway design. It is for the first time that a GMCR-plus model is applied for conflict resolution in the optimal design of the stepped spillway. Table 1 provided a summary of the studies on optimizing the spillway design.

Table 1
Summary of relevant studies on optimizing the spillway design.

Hydraulic structure	Optimization method	Objectives	Findings	Ref
Cascade spillway	Genetic Algorithm (GA), Gravitational Search Algorithm (GSA), Particle Swarm Optimization (PSO), and Artificial Bee Colony (ABC)	minimizing the construction cost	effectiveness of these algorithms to optimize cascade spillway design	[31]
Stepped spillway	GA	minimizing the total cost of the stepped spillway and downstream dissipaters	GA efficiency for spillway optimization	[52]
Stepped spillways	Particle swarm optimization-based least square support vector machine (PSO-LSSVM)	recognize the factors affecting the discharge coefficient and energy dissipation and finding the best possible estimation of hydraulic parameters	PSO-LSSVM is accurate for the prediction of the discharge coefficient and energy dissipation over the spillway	[53]
Stepped spillways	Honey-bee mating optimization (HBMO) algorithm	minimizing the total cost of spillway chute and stilling basin	high potential of the HBMO in spillway design	[39]
Stepped spillways	Improved artificial bee colony (IABC) and improved particle swarm optimization (IPSO)	minimizing the construction costs	these proposed methods are highly recommended for solving large-scale problems that cost and computational efforts are vital for the optimal design	[40]
Stepped spillway	Nondominated sorting genetic algorithm II (NSGA-II)	maximizing the energy dissipation and cavitation number, and minimizing the construction cost	the uncertainty of flood flow over the stepped spillway change spillway geometry	[3]
Stepped spillway	NSGA-II	maximizing energy dissipation and minimizing construction cost	the more the stairs' height, the more energy dissipation	[33]
Chute-Flip Bucket (CFB) system	GA	optimizing the geometry of the CFB system	the optimal design increased the cavitation index and energy dissipation by 30 and 32%	[19]
Modified horseshoe spillway (MHS) and classical horseshoe spillway (CHS)	Cubic polynomial models	to determine the optimal geometric design	higher discharge efficiencies in MHS occur at low water heads and high internal to external weir lengths	[54]
Ski-jump spillway	ANN-HHO (Harris hawks optimization), ANN-PSO (particle swarm optimization) model, and ANN-GA model	to predict the scour depth (SD) downstream of the ski-jump spillway	ANN-HHO is efficient for SD prediction in the ski-jump spillway	[32]
Labyrinth spillway (LS)	Differential Evolution (DE) algorithm and GA	minimizing the construction costs (structural volume)	optimization algorithms are useful for the design of LS	[34]
Labyrinth spillway (LS)	Shuffled frog leaping algorithm (SFLA)	the best geometry of spillway under climate change impacts	design flood highly affects spillway geometry, and the optimization model is very effective for reducing construction costs.	[36]
Labyrinth spillway	Hybrid of particle swarm optimization, gray wolf optimization (GWO), and direct search optimization meta-heuristic approach	minimizing the construction costs (the total volume of spillway body)	the hybrid of meta-heuristic algorithms are highly efficient for the optimal design of the Labyrinth spillway	[38]
Ogee-Crested Spillway	GA and regression model	minimizing the construction costs	GA is relatively effective	[35]
free-flow, stepped, semicircular and cylindrical spillways	Harmony Search Algorithm (HSA)	optimizing the type and geometry of the spillway	meta-heuristic algorithms are efficient for spillway design, and economy affects optimal dimensions of the spillway	[37]

(*continued on next page*)

Table 1 (*continued*).

Hydraulic structure	Optimization method	Objectives	Findings	Ref
Spillway	Direct search method	optimal spillway capacity and dimensions considering uncertainties in estimating flood magnitude and flood routing process	The flood uncertainty is essential in spillway design	[45]
Spillway of embankment dam	Log Pearson type III (LP3) and the three-parameter lognormal (LN3) distribution	optimum spillway capacity considering the uncertainty in the flood magnitude estimation	Considering the uncertainty in the flood magnitude can highly change the optimal spillway design	[44]

3. Material and methods

The suggested approach involves five steps, including data collection (step 1), numerical simulation (step 2), developing MLP-ANN surrogate model (step 3), risk-based optimization model (step 4), and graph model for conflict resolution (step 5) as illustrated in Fig. 1.

3.1. Data gathering

Jarreh Dam reservoir was constructed over the Zard River in southern Iran. The flood discharge system of this dam has two main gated and emergency stepped spillways. The stepped spillway consists of three sections with different lengths that are shown in Fig. S1 of Electronic Supplementary Material (ESM), along with the stepped spillway characteristics. The geometrical features and experimental data from the small-scale physical model (implemented by Khuzestan Water and Wastewater Company; KWPA) were used to develop, calibrate, and validate the FLOW-3D® model. For this purpose, the water flow depth and velocity were measured for nine cross-sections, each one including five points ($9\times5 = 45$) over the stepped spillway of the experimental model for two different flow rates (2000 and 2300 m^3/s).

The conflicts between the project owner and the designer (the main decision-makers) over the optimal design of the stepped spillway were investigated in this study. While the designer's primary concern was achieving a design plan with the highest hydraulic performance (defined with cavitation number and energy dissipation), the project owner's priority was minimizing the cost (defined as the concrete volume). Achieving a design plan that provides maximum hydraulic performance and minimum cost simultaneously was difficult and could raise a conflict between the designer and the project owner.

3.2. Developing the flow simulation model

According to the proper potential of the RHINOCEROS® software, it was utilized to design the three-dimensional stepped spillway model (Fig. S2 in ESM). Then, FLOW-3D®, as a general model with 3D analysis capability in computational fluid dynamics (CFD) problems [14], was selected to conduct a flow simulation in the stepped spillway (Fig. S3 in ESM). FLOW-3D® model applies three-dimensional continuity and momentum equations in numerical modeling of incompressible flow, which at three-dimensional Cartesian coordinates are presented by Eqs. (1) and (2).

$$v_F\frac{\partial \rho}{\partial t}+\frac{\partial}{\partial x}\left(uA_x\right)+\frac{\partial}{\partial y}\left(vA_y\right)+\frac{\partial}{\partial z}\left(wA_z\right)=\frac{RSOF}{\rho} \quad (1)$$

where, (u, v, w) is velocity components in the coordinate directions (x, y, z), A_x, A_y, A_z are cross-sectional area open to flow in the coordinate directions (x, y, z), ρ shows fluid density; RSOR and v_F indicate the source term and the fluid volume fraction, respectively.

$$\frac{\partial u}{\partial t}+\frac{1}{V_F}\left(uA_x\frac{\partial u}{\partial x}+vA_y\frac{\partial u}{\partial y}+wA_z\frac{\partial u}{\partial z}\right)=-\frac{1}{\rho}\frac{\partial p}{\partial x}+G_x+f_x \quad (2a)$$

$$\frac{\partial v}{\partial t}+\frac{1}{V_F}\left(uA_x\frac{\partial v}{\partial x}+vA_y\frac{\partial v}{\partial y}+wA_z\frac{\partial v}{\partial z}\right)=-\frac{1}{\rho}\frac{\partial p}{\partial y}+G_y+f_y \quad (2b)$$

$$\frac{\partial w}{\partial t}+\frac{1}{V_F}\left(uA_x\frac{\partial w}{\partial x}+vA_y\frac{\partial w}{\partial y}+wA_z\frac{\partial w}{\partial z}\right)=-\frac{1}{\rho}\frac{\partial p}{\partial z}+G_z+f_z \quad (2c)$$

where p is fluid pressure, $G_{(x,y,z)}$ the acceleration resulted from body fluids in the coordinate directions (x, y, z); $f_{(x,y,z)}$ viscosity acceleration at three dimensions, and V_F a fractional volume open to flow [55,56]. FLOW-3D® model solves governing equations using a finite difference method along with a Fractional Area and Volume Obstacle Representation (FAVOR) method. FLOW-3D® model adopts a Hirt–Nichols' volume of fluid (VOF) [57] by means of the fixed Eulerian method to calculate the free water surface, which is the boundary between water and air [55,56]. VOF and FAVOR are a part of the finite volume method in the FLOW-3D® model and divide the modeling area into a network of smaller elements or controlling volume. For detailed information regarding the FLOW-3D® model, readers can refer to [55,56].

The mesh size is of great importance in flow simulation, and therefore the elements' dimension should be selected so that the model becomes stable. One effective method for determining optimum cell dimensions is to define a model with a relatively large network dimension and then gradually reduce the dimensions to achieve the desired output value. This reduction is continued so that the changes in results cannot be achieved in smaller grids. The FLOW-3D® model was executed for three different mesh sizes (i.e., $80\times80\times30$, $60\times60\times30$, and $30\times30\times30$ cm). In the FLOW-3D® model, the type of cells and their mesh size are significant factors considering the boundary cells. In this study, one meshing block was applied to define the boundary conditions, in which the bed floor and sides of the meshing block were considered as the wall. This virtual wall in boundary conditions is used to compute effective shear stress at the wall [58]. After determining the suitable mesh size (by sensitivity analysis), flow simulations were performed for various boundary conditions, and the best condition was chosen by sensitivity analysis and comparing the experimental data with the results of the numerical simulation.

Moreover, the flow turbulence model is another effective factor in the FLOW-3D® simulation model. In this study, three turbulence models, including the k-ε model [59], the RNG (Renormalized Group) k-ε model [60], and the LES (Large Eddy Simulation) model [61] were utilized to describe the flow turbulence in FLOW-3D®. The roughness of the boundaries is an essential issue in CFD models because it could affect the energy dissipation [62]. Roughness coefficients (with the dimensions of length) are usually defined by Chezy's resistance coefficient or Manning's n parameter [58]. The roughness is better to be smaller than

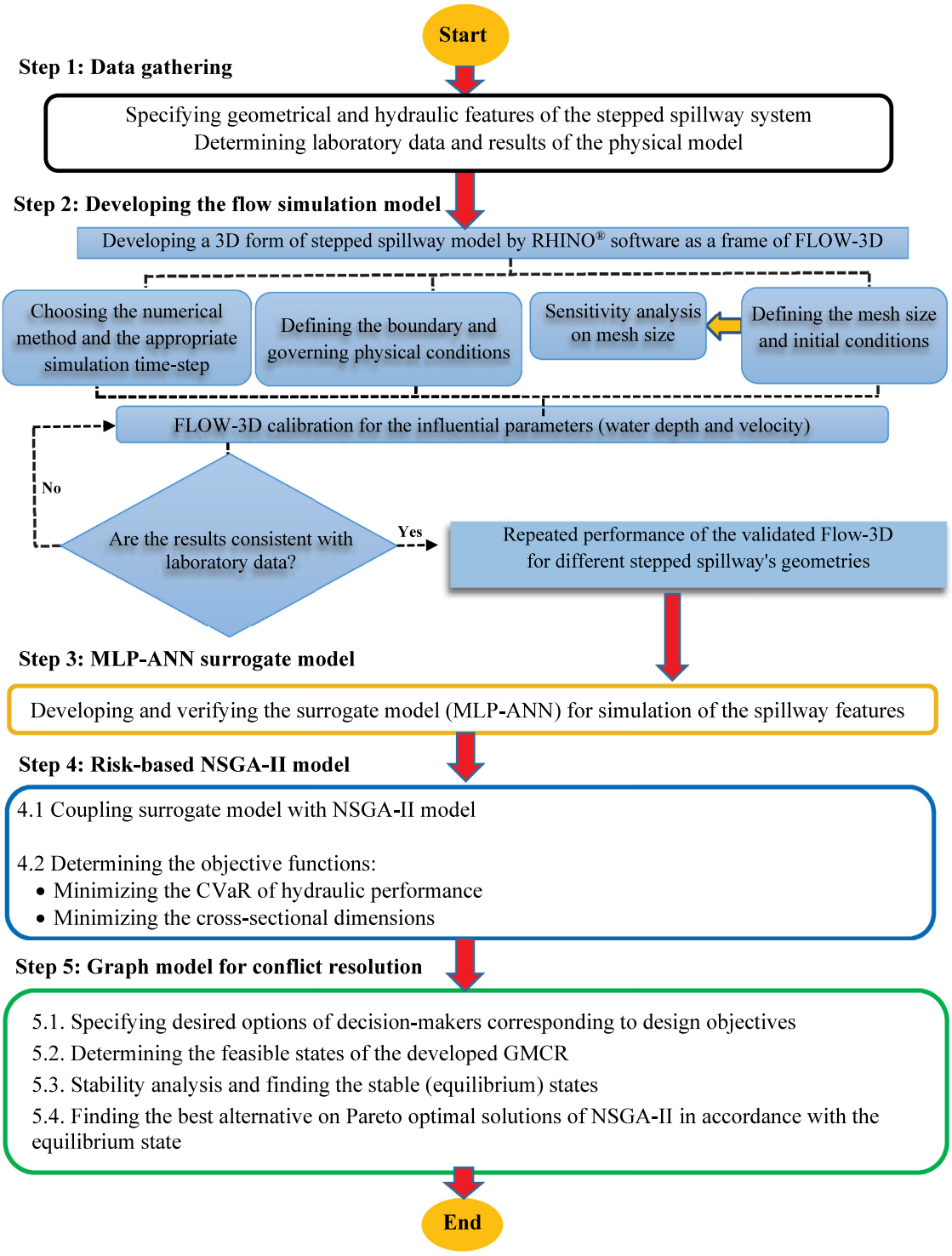

Fig. 1. The main steps of the suggested approach for optimal spillway design.

the grid cell size at the boundaries [62,63]. The incorporation of roughness into FLOW-3D® was accomplished by adopting the average height of surface imperfections as a uniform surface roughness for the desired components. In the present study, the FLOW-3D® model was executed for probable roughness scenarios (i.e., the roughness of concrete, glass, and without roughness) to assess the effect of roughness on flow characteristics and find the best roughness for numerical simulation. The information about the mesh network, boundary conditions, and turbulence models is illustrated in Table S1 (ESM). Also, the results of sensitivity analysis on turbulence models, roughness, and mesh size are presented in section S1 of ESM (Figs. S6–S8, and Tables S2–S4).

Finally, the model was calibrated for depth and velocity of water flow as the most influential hydraulic parameters on physical conditions. The depth and velocity of water flow on the stepped spillway were recorded in nine sections and totally for 45 points (Fig. S1 in ESM) of the experimental model, which provided an accurate comparison between the simulations of FLOW-3D® and

the results of the laboratory model (Fig. S5 in ESM). It is notable that five different flow rates (500, 1000, 1500, 2000, and 2300 m^3/s) were applied in the experimental model; however, this study only presents the flow rate of 2000 and 2300 m^3/s. This decision was mainly related to the utmost effect of high flow rates on energy dissipation and cavitation risk.

3.3. MLP-ANN surrogate model

There were some difficulties in coupling the FLOW-3D® model to the optimization model [3]. Hence, an MLP-ANN surrogate model was employed as the replacement of the numerical flow simulation on the stepped spillway. For big data from a dynamic system with unknown fundamental physical relationships, the Artificial Neural Network (ANN) was used to specify the relationship between input and output variables [64]. This replacement aims to achieve a model with less runtime and the capability of linking with the optimization model [65]. Hence, in the third step, the validated Flow-3D® model was repeatedly implemented for 96 potential scenarios with various geometries (e.g., length and height of spillway, and the steps' number) and two different flow rates (i.e., 2000 and 2300 m^3/s). In all 192 runs of the FLOW-3D® model, energy dissipation (between the beginning and the end of the spillway in all 192 design scenarios) and cavitation number (in all steps of the spillway, 192 × 6) were recorded. The obtained data were used as the required input–output data for developing the MLP-ANN surrogate model. Notably, based on a sensitivity analysis, the entire data, in a proportion of one (25%) to three (75%), were used for training and testing phases. A different number of neurons in the hidden layer and transfer functions were evaluated, and the minimum statistical errors (e.g., Mean Absolute Relative Error (MARE), Sum of Squared Errors (SSE), coefficient of determination (R^2), and Mean Squared Error (MSE)) were obtained in a neural network with three layers and eight neurons for the hidden layer. The training function in the MLP-ANN model was Levenberg–Marquardt with feedforward networks for simple processing units.

3.4. Risk-based NSGA-II model

In this study, a risk-based optimization model was utilized to minimize the risk of poor hydraulic performance and construction cost. The optimization algorithm was NSGA-II, which provides a variety of alternatives on Pareto and maintains the solution proximal to the right Pareto optimal set [66].

3.4.1. Risk assessment

The risk assessment was considered in the optimization model through conditional value at risk (CVaR). Each coherent risk measure method (e.g., σ) should satisfy some axioms, including Monotonicity (Eq. (3)), Translation Equivariance (Eq. (4)), Subadditivity (Eq. (5)), and Positive Homogeneity (Eq. (6)) [67]. For random variables x and y, descriptions of these axioms are presented as follow:

$$x \le y \rightarrow \sigma(y) \le \sigma(x) \tag{3}$$

$$C \in R \rightarrow \sigma(x + C) = \sigma(x) + C \tag{4}$$

$$\sigma(x + y) \le \sigma(x) + \sigma(y) \tag{5}$$

$$h \ge 0 \rightarrow \sigma(hx) = h.\sigma(x) \tag{6}$$

Monotonicity expresses that the higher losses, the higher risk. Translation Equivariance declares that an increase (decrease) like C in loss makes the same increase (decrease) in the risk. Subadditivity remarks variety reduces risk, and Positive Homogeneity notes that the risk is doubled by doubling the portfolio size.

The value-at-risk (VaR) and CVaR are defined as the maximum loss with a given confidence level β (a certain level of cumulative probability), and the expected value of the loss that exceeds VaR (or mean excess loss), respectively. CVaR as a coherent risk measure function satisfies all four axioms and indicates the conditional value-at-risk at confidence level β [68]. Accordingly, assuming $z = f(x, y)$ to be the distribution function of losses related to decision vector $x \in X$ and random vector $y \in Y$; the cumulative distribution function $\Psi(x, z)$ would be defined as Eq. (7). Therefore, VaR and CVaR at the confidence level of $\alpha \in [0, 1]$ are defined by Eqs. (8) and (9), respectively.

$$\Psi(x, z) = P\{y | f(x, y) \le z\} \tag{7}$$

$$VaR_\beta(x) = \min\{z | \Psi(x, z) \ge \beta\} \tag{8}$$

$$CVaR_\beta(x) = E\{z | \Psi(x, z) \ge \beta\} \tag{9}$$

where, P and E refer to probability function and expected value operator, respectively. When a limited number of scenarios (S) at particular confidence level β represent the y, minimizing the following function in Eq. (10) over x and v delivers the CVaR [28,69].

$$F_\beta(x, v) = v + \frac{1}{(1-\beta)} \sum_{s=1}^{S} max\{0, f(x, s) - v\} p(s) \tag{10}$$

where v is equivalent to VaR and $p(s)$ is the probability of scenario s.

3.4.2. Developing NSGA-II model

The optimization model was developed by coupling the multi-objective NSGA-II optimization model and the validated surrogate model (MLP-ANN). The risk-based NSGA-II model attempts to (1) minimize the risk of poor hydraulic performance (a combination of cavitation number and energy dissipation) (Eq. (11)) using the CVaR measure, and (2) minimize the construction cost in the form of cross-sectional dimensions (calculating the volume of needed concrete) (Eq. (14)). The CVaR, known as a coherent risk measure, was used here to calculate the hydraulic performance according to the worst-case flood flow rate scenarios. The formulation of the developed optimization model to get Pareto optimal solutions is as follows:

$$Min\ f_1 = CVaR^\beta_{HP} = 0.6\left(\frac{CVaR_{Cav}}{10.9\,(N) \times 2(N)}\right) + 0.4\left(\frac{CVaR_{\Delta E}}{3.61}\right) \tag{11}$$

$$CVaR_{Cav} = VaR^\beta_{Cav} + \frac{1}{1-\beta} \sum_{s=1}^{S} \left[Cav_s^{loss} - VaR^\beta_{Cav}\right] \times p(s) \tag{12}$$

$$\left[Cav_s^{loss} - VaR^\beta_{Cav}\right] = \begin{cases} Cav_s^{loss} - VaR^\beta_{Cav} & if\ Cav_s^{loss} > VaR^\beta_{Cav} \\ 0 & otherwise \end{cases}$$

$$Cav = \frac{2(p_0 - p_v)}{\rho v^2}$$

$$CVaR_{\Delta E} = VaR^\beta_{\Delta E} + \frac{1}{1-\beta} \sum_{s=1}^{S} \left[\Delta E_s^{loss} - VaR^\beta_{\Delta E}\right] \times p(s) \tag{13}$$

$$\left[\Delta E_s^{loss} - VaR^\beta_{\Delta E}\right] = \begin{cases} \Delta E_s^{loss} - VaR^\beta_{\Delta E} & if\ \Delta E_s^{loss} > VaR^\beta_{\Delta E} \\ 0 & otherwise \end{cases}$$

$$\Delta E_i = \frac{E_2 - E_1}{E_1}$$

$$Min\ f_2 = (-3557.29) + \left(1229.51 \times H_{sp}\right) + \left(256.75 \times W_{sp}\right) + (82.75 \times N) \tag{14}$$

Subject to

$$\Delta E = f(w_s, h_s, H_{sp}, w_{sp}) \tag{15}$$

$$Cav = f(p_0, p_v, \rho, v) \tag{16}$$

$$2.5 \leq H_{sp} \leq 4 \quad (17)$$

$$10 \leq W_{sp} \leq 15 \quad (18)$$

$$4 \leq N \leq 8 \quad (19)$$

$CVaR^{\beta}_{HP}$ (Eq. (11)) is the conditional value at risk on β confidence level for losses of hydraulic performance in the stepped spillway, which is determined as the sum of $CVaR_{Cav}$(CVaR of cavitation, Eq. (12)) and $CVaR_{\Delta E}$ (CVaR of energy dissipation, Eq. (13)) with different factors in reference to the opinion of local authorities. VaR^{β}_{Cav} and $VaR^{\beta}_{\Delta E}$ are the value at risk (or the maximum loss on confidence level β) for cavitation and energy dissipation, respectively. Cav_s^{loss} and ΔE_s^{loss} indicate the loss generated by cavitation and energy dissipation in scenario $s \in S$. As shown by Eq. (15), the energy dissipation (ΔE), in a stepped spillway is a function of spillway height (H_{sp}) and width (W_{sp}), and the steps' height and width (h_s and w_s). Notably, in Eq. (13), E_2 and E_1 stand for the downstream and upstream energy of spillway (with units of velocity squared per second m^2/s^3), respectively. Also, the cavitation number (Cav) in Eq. (16) acts as a function of ρ (fluid density), v (calculated flow velocity by FLOW-3D® model), p_0 (local absolute pressure), and p_v (the flow pressure). Notably, a linear multivariable regression (Eq. (14)) was used to calculate the required concrete volume for the construction of the stepped spillway, in which CV shows the concrete volume, which in turn depends on H_{sp}, W_{sp}, and the number of steps (N). The variation range of geometrical parameters (Eqs. (17)–(19)) were assumed based on the field information to approach the real situation in the stepped spillway of the Jarreh Dam.

The parameters of the risk-based optimization model were selected by a sensitivity analysis to reassures that the general (global) optimum is reached. Based on sensitivity analysis, for the risk-based NSGA-II optimization model, the best values for generation, population size, and mutation and crossover rates were 250, 30, 0.1, and 0.9, respectively. Also, the Hypervolume metric [70–72] as a well-known performance measure was used to verify the performance of the risk-based NSGA-II optimization model. The Hypervolume (HV) applies both convergence and diversity to return a combined qualitative measure of algorithm performance [73]. Assuming a problem in which all objectives must be minimized, the lower the value of this criterion, the more desirable the algorithm. Based on this metric, in this study, as the generation number increases, the HV value decreases. The decreasing trend continues until the generation number of 250, and then, HV converges to an acceptable value (0.19), representing that variation in final optimized answers after this number of generations was insignificant. The optimization model results in Pareto optimal solutions considering objectives and provides a comprehensive view of decision-making [3].

3.5. Graph model for conflict resolution

NSGA-II cannot select a comprehensive solution considering the priority of decision-makers [66]. The objectives of the optimization model are conflicting. In the design of stepped spillways, improving the hydraulic performance necessitates apparent cross-sectional dimension increases, which may cause financial concerns for the project owner. Therefore, the compromise solution on the Pareto optimal solutions was selected based on the conflict between the designer and project owner. The project owner-designer conflict was modeled by the GMCR theory using the GMCR-plus decision support system. The GMCR resolves the real-world conflicts based on the concept of game theory, in which decision-makers are allowed to move in any possible order. GMCR-plus is the latest GMCR computerized decision support system (followed by GMCR-I and GMCR-II) that facilitates the understanding of the conflict [29]. The developed GMCR model contains two main stages of modeling and stability analysis [74].

3.5.1. The modeling stage

First of all, the conflict involved decision-makers (e.g., designer and project owner), and their strategies (options) were defined. After defining the options of decision-makers, all infeasible states (impossible conditions) were omitted by two methods, namely "Remove as Mutually Exclusive Options" and "Remove as Infeasible Condition". After that, the irreversible movements of each decision-maker and relative preferences of the states for decision-makers were determined to rank the states [74].

3.5.2. The analysis stage

In this stage, after preference ranking, the equilibrium state (a stable state for both decision-makers) for each decision-maker was achieved based on the stability definitions (solution concepts). GMCR uses four main solution concepts, including Nash stability [75], general metarationality (GMR) [76], symmetric metarationality (SMR) [76], and sequential stability (SEQ). These stability definitions vary in their level of foresight, willingness to disimprovement, knowledge of preferences, and strategic risk and consequently represent different behavior of decision-makers with various preferences [77,78].

4. Results

4.1. Numerical simulation

To verify the numerical simulation, the experimental information was compared with the output of the numerical simulation in different scenarios of turbulence models, material type (roughness), and mesh size. Fig. S6, as well as Table S2 in ESM, show the results of sensitivity analysis on mesh size in simulating the depth and velocity of water flow. Regarding the error-index (MARE) and the run time of the FLOW-3D® model, the size of ($60 \times 60 \times 30$) was chosen as the best mesh alternative. Different turbulence models (i.e., k–ϵ, RNG, and LES) were used in numerical simulation, and the results were compared with the experimental data from the small-scale physical model of Jarreh spillway regarding depth and velocity of water flow (Fig. S7). The result of the MARE error index for different turbulence models is presented in Table S3 in ESM, in which the LES turbulence model shows the best match with the experimental data. Also, Fig. S8 presents the sensitivity analysis on the roughness of the boundaries, and Table S4 (ESM) indicates the MARE index for depth and velocity of water flow regarding various roughnesses. Based on Table S4, the FLOW-3D® simulation model developed by glass roughness resulted in the least error values.

4.2. MLP-ANN surrogate model

The surrogate model was developed using data from the repeated performance of the numerical simulation. The effectiveness of the surrogate model (MLP-ANN) in estimating the cavitation number and energy dissipation is indicated in Fig. 2. As shown in Fig. 2a and b, the surrogate model captured the general trend and was very helpful in estimating the values of energy dissipation in a probabilistic manner. Also, based on Fig. 2c and d, the surrogate model had good performance over the high as well as the low amount of cavitation number. Table 2 demonstrates the model performance in the validation phase, given different error indices. It is obvious that the model had good performance in predicting the energy dissipation ($R^2 = 98\%$) and cavitation number ($R^2 = 98.3\%$).

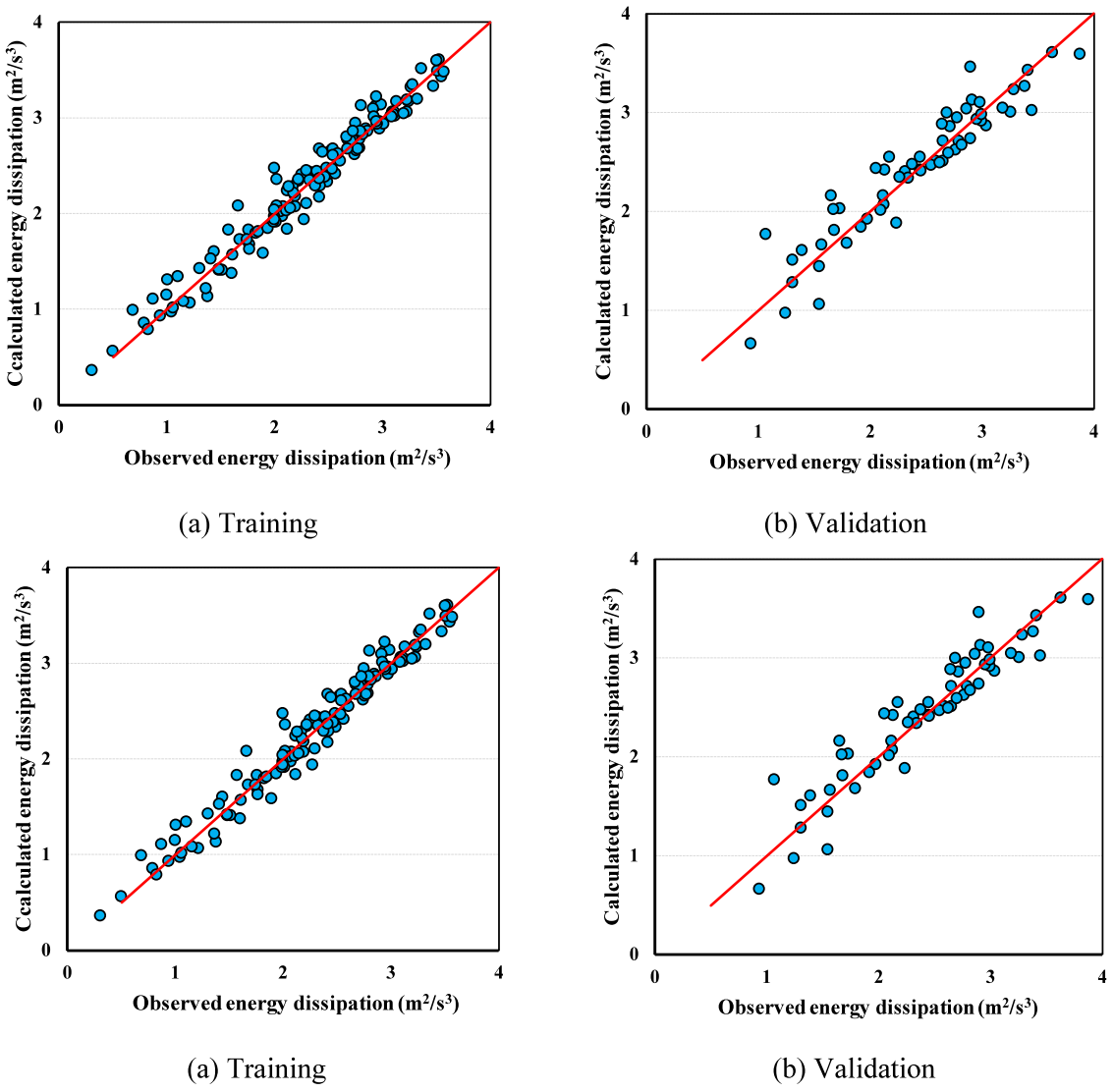

Fig. 2. The effectiveness of the surrogate model (MLP-ANN) for energy dissipation (a and b) and cavitation number (c and d).

Table 2
Performance of surrogate model (MLP-ANN) in the validation phase.

Parameter	Type of error index			
	MARE (%)	MSE	SSE	R^2
Energy dissipation	7.65	0.30	88.84	0.9802
Cavitation number	6.35	0.26	76.51	0.9830

4.3. Finding the optimal solution by NSGA-II

The risk-based optimization model was developed through coupling the MLP-ANN and NSGA-II based optimization model for two objectives, including (1) minimizing the CVaR of hydraulic performance (a combination of energy dissipation and cavitation risk) (Eq. (11)), which is the designer concern, and (2) minimizing the construction cost in the form of cross-sectional dimensions (the volume of needed concrete) (Eq. (14)) as the concern of project owner. The risk-based optimization model resulted in the Pareto optimal solutions with 20 unique design scenarios (Fig. 3). Table 3 presents the geometrical features and corresponding objectives values for optimal solutions obtained from the risk-based optimization model.

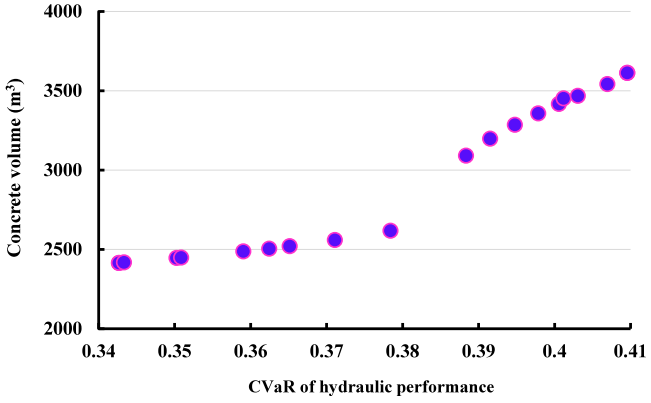

Fig. 3. Pareto optimal solutions obtained by the risk-based optimization model.

4.4. Conflict resolution by GMCR

To achieve the final design alternative among the Pareto optimal solutions, the conflict between the project owner and the designer should be addressed. In this conflict, the project owner

Table 3
The geometrical features and corresponding objectives values for optimal solutions.

Solution number	Spillway geometry*			Objective values	
	H_{sp} (m)	L_{sp} (m)	No. of steps	$CVaR_{HP}^{\beta}$	CV (m^3)
1	2.5	10	4	0.34	2415
2	2.5	10	4	0.34	2415
3	2.5	10.01	4	0.34	2418
4	2.5	10.12	4	0.35	2446
5	2.5	10.13	4	0.35	2448
6	2.5	10.28	4	0.36	2487
7	2.5	10.35	4	0.36	2505
8	2.5	10.41	4	0.37	2520
9	2.5	10.56	4	0.37	2559
10	2.5	10.79	4	0.38	2618
11	2.5	12.63	4	0.39	3090
12	2.5	13.05	4	0.39	3198
13	2.5	13.39	4	0.39	3285
14	2.5	13.67	4	0.40	3357
15	2.5	13.9	4	0.40	3416
16	2.51	13.99	4	0.40	3452
17	2.5	14.1	4	0.40	3468
18	2.5	14.39	4	0.41	3542
19	2.52	14.57	4	0.41	3613
20	2.52	14.57	4	0.41	3613

Note: * H_{sp} (m) and L_{sp} (m) show the spillway's height and length, respectively. $CVaR_{HP}^{\beta}$ shows the risk of poor hydraulic performance (a combination of cavitation number and energy dissipation) (Eq. (11)), and CV shows the construction cost in the form of cross-sectional dimensions (volume of needed concrete) (Eq. (14)).

and the designer had different perspectives. From the designer point of view and based on the values of the first objective (Eq. (9)), the alternatives of stepped spillway design were classified into three groups, including (i) low-cost design, in which the designer tries to minimize the construction cost, which may not necessarily lead to the best hydraulic performance; it means that the designer prioritizes the construction cost to the hydraulic performance, (ii) reasonable design that the designer considers both hydraulic performance and construction cost in the design process and tries to make a balance between them, and (iii) conservative design, in which regardless of the construction cost, the designer desires to achieve the best hydraulic performance of the stepped spillway. Given the values of required concrete volume (Eq. (12)), the project owner could have three alternatives, including (i) hiring a third-party consultant for strict cost supervision, (ii) asking for a financial report to check the project costs and the details of design and comparing the possible alternatives, and (iii) accept the proposed design without further investigations. These categories are presented in Table 4.

It should be noted that the decision-makers' strategies (options) were assumed given the social, economic, climatic, technical, and financial constraints of the project to achieve the most compatible state with regional conditions. Then, considering these constraints, the objective values in Table 3 were classified for the options of the project owner and the designer (see Table 5). Table 5 shows that the project owner can accept the design plan regardless of the cost (concrete volume), corresponding to solution # 1–20. However, sometimes due to financial limitations such as allocated budget, the project owner should make a limitation in cost. Hence, the project owner can request a report for the design to limit the cost in a desirable range (i.e., $0 < CV < 2500$, corresponding to solution # 1–6), or even in a stricter mode, hire a consultant team to monitor the cost and achieve the minimum value (i.e., $0 < CV < 2420$, corresponding to solution # 1–3). On the other hand, if the designer could deliver a plan with $0.4 < CVaR_{HP}$ it is a conservative design in which, regardless of the required cost for construction, the designer focuses on the stepped spillway's hydraulic performance. Also, the design with $0.35 < CVaR_{HP} < 0.4$ is a reasonable design, in which the construction cost is considered in addition to hydraulic performance, and for $CVaR_{HP} \leq 0.35$ it would be a low-cost design in which the construction cost is prioritized to hydraulic performance.

For removing the infeasible states, the options in Table 4 (i.e., "Consultant", "Reports", and "Acceptable design" for the project owner and also, "Low-cost", "Reasonable design", and "Conservative design" for the designer) are mutually exclusive, and each decision-maker should select only one state. Therefore, 41 states (out of 64) are infeasible. Furthermore, each decision-maker would take at least one option, and 14 states (in which decision-makers may choose no option) are infeasible. Additionally, it is impossible for two extreme states (the best state for the decision-maker) to occur simultaneously. Thus, achieving the conservative design (the best hydraulic performance) is possible only when the project owner accepts all construction costs. As a result, two states, including having a conservative design when the project owner asks for a report or uses a third-party consultant for supervision, cannot occur. Also, hiring a third-party consultant for supervision is only justified if it leads to the lowest cost design. Hence, one more state, which is having a consultant to supervise the design and getting a reasonable design, is not feasible. Totally $41+14+3 = 58$ states (out of 64) were removed. The remaining six states are presented in Table 6.

The preference of the decision-makers on the feasible states is shown in Table 7, in which the project owner desires to accept the provided design if the designer accept to deliver a low-cost design (state # 4) as the most preferred alternative and after that, the best state for the project owner would be asking for the report on the provided low-cost design (state # 3).

On the other hand, the best state for the designer would be delivering a conservative design that is accepted by the project owner (state # 1) and then delivering a reasonable design that is accepted by the project owner (state # 6). Besides, state #1 (a conservative design, accepted by the owner) and # 2 (a low-cost design, which has to be supervised by a consultant) were ranked as the least preferred options for the project owner and the designer, respectively. After preference ranking, the equilibrium state for each decision-maker was reached by stability analysis and four main stability definitions (solution concepts), including SMR, Nash, SEQ, and GMR. The results of the stability analysis are presented in Table 8.

Table 4
The options of the project owner-designer conflict for the design of stepped spillway.

DM[a]	Options
Project owner	Hiring a third-party consultant for strict cost supervision (Consultant) Requesting for financial reports to check the costs and details (Reports) The costs are acceptable without further investigations (Acceptable design)
Designer	A design with minimum possible cost (Low-cost design) A design with a reasonable cost and performance (Reasonable design) A design with maximum possible cavitation index and energy dissipation (Conservative design)

[a]DM: decision-maker.

Table 5
Classification of objective values based on the options of project owner-designer conflict.

	$CVaR_{HP}^{\beta*}$	Designer options		CV**	Project owner options
1	0.34	Low-cost design	**1**	2415	Consultant
2	0.34		**2**	2415	
3	0.34		**3**	2417	Reports
4	0.35		**4**	2445	
5	0.35		**5**	2448	
6	0.36	Reasonable design	**6**	2486	
7	0.36		**7**	2504	Acceptable design
8	0.37		**8**	2520	
9	0.37		**9**	2558	
10	0.38		**10**	2617	
11	0.39		**11**	3090	
12	0.39		**12**	3198	
13	0.39		**13**	3285	
14	0.40	Conservative design	**14**	3357	
15	0.40		**15**	3416	
16	0.40		**16**	3451	
17	0.40		**17**	3467	
18	0.41		**18**	3542	
19	0.41		**19**	3612	
20	0.41		**20**	3612	

*$CVaR_{HP}^{\beta}$ shows the risk of poor hydraulic performance (a combination of cavitation number and energy dissipation) (Eq. 11). and ** CV (m^3) shows the construction cost in the form of cross-sectional dimensions (volume of needed concrete) (Eq. 14).

Table 6
The feasible states for the developed GMCR (project owner-designer conflict)

DM[a]	Options	Feasible states					
		1	2	3	4	5	6
Project owner	Consultant	N[b]	Y[c]	N	N	N	N
	Reports	N	N	Y	N	Y	N
	Acceptable	Y	N	N	Y	N	Y
Designer	Conservative	Y	N	N	N	N	N
	Low-cost	N	Y	Y	Y	N	N
	Reasonable	N	N	N	N	Y	Y

[a]DM: Decision-maker.
[b]N: No.
[c]Y: Yes.

Table 7
Ranking of the feasible states for project owner and designer.

DM[a]	States					
	Most preference				Least preference	
Owner	4	3	2	5	6	1
Designer	1	6	5	4	3	2

[a]DM: Decision-maker.

The stability analysis indicates that states # 1 and # 5 are the equilibria states selected by all stability definitions. Fig. 4 visually shows these equilibria results as an integrated graph, in which arrows represent the unilateral improvements. As shown in Fig. 4, state # 1 would be a stable state when states # 4 and # 6 happen. The common feature of states # 4 and # 6 is that the project owner accepts the designer's plan without any further investigations, and in response, the designer delivers a low-cost design (state # 4) or reasonable design (state # 6). Also, state # 5 would be a stable state when states # 3 and # 6 occur. It is important to note that the owner is more likely to accept state # 5 since the project owner has a direct unilateral improvement to this state (Fig. 4).

Table 8
Stability analysis and equilibria results.

Stability definition	State number					
	1	2	3	4	5	6
Nash[a]	Y				Y	
GMR[b]	Y	Y			Y	
SMR[c]	Y	Y			Y	
SEQ[d]	Y	Y			Y	

[a]Nash: Nash stability.
[b]GMR: general metarationality.
[c]SMR: symmetric metarationality.
[d]SEQ: sequential stability.

Accordingly, the project owner and the designer are more likely to agree on state # 5 as the best possible equilibrium, in which the project owner agrees to reasonable design, and the designer agrees to deliver a design with a financial report. The possible alternatives on the Pareto optimal solutions (Table 5) for the reasonable design were solutions # 6–13, and for the design with the report were solutions # 1–6. Therefore, solution # 6 was the compromise solution for the conflict between the project owner and the designer.

5. Discussion

The considerable impact of the flood flow uncertainty on the hydraulic operation of spillways necessitates investigating the risk of flood flow uncertainty in the optimal spillway design. Various small-scale physical models [6–11] and computational fluid dynamics (CFD) modeling [56,79,80] have been utilized for risk assessment and evaluating the efficiency of an existing structure. However, the high cost of physical models and the time-consuming nature of numerical simulation models prevents evaluating the effect of a sufficient number of possible flood flow scenarios on the designed optimal stepped spillway.

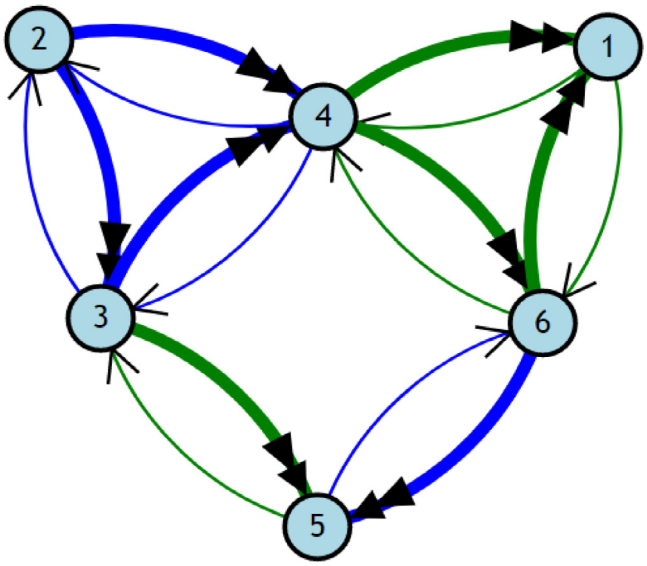

Fig. 4. The equilibria result of GMCR-plus in graph form for only unilateral improvements (UIs), Blue: project owner, green: designer. (Note: the figure is adapted from the GMCR-plus model.)

Hence, the application of a risk-based method was assessed in this study to reliably evaluate the effect of flood uncertainty on the hydraulic performance of stepped spillways and eliminate the existing shortcomings in the literature. The developed risk-based optimization framework, relying on the validated data from a physical model and the numerical simulations (by FLOW-3D® model), attempted to determine an economical design scenario with the minimum loss in hydraulic performance. Also, social complexities in the form of different perspectives of the decision-makers (i.e., project owner and designer) were considered by GMCR-plus to obtain a compromise optimal spillway design.

The suggested method provides a cost-effective design scenario with minimum loss in hydraulic performance due to flood flow risk. Regarding the previous studies, Mooselu et al. 2019 [3] suggested a simulation–optimization approach for the stepped spillway design in the same case study. In their study, the flood flow uncertainty in the stepped spillway was analyzed using the fuzzy transformation method that provided the best scenarios for spillway geometry in various α-cut levels. The upper and lower limits of the optimal scenarios were determined by two decision models, i.e., PROMETHEE and TOPSIS. Our results in the selected scenario (#6) with the spillway length of 10.28 m and height of 2.5 m (see Table 3) are entirely consistent with the proposed range in [3] for length (10–14.9 m) and height (2.5–2.8 m) of the stepped spillway in different α-cut levels, resulted from PROMETHEE model. Application of the fuzzy transformation method to consider the flood flow uncertainty in their work resulted in a range for the geometrical parameters of the spillway in different α-cut levels, while the risk-based multi-objective optimization model in this study suggested more accurate values for the spillway geometry in the selected scenario. In addition, the developed design scenario, which is a compatible scenario with the region's conditions, satisfies the desires of regional stakeholders and facilitates the construction and operation phases.

Regarding the limitations of the proposed methodology in this research, it should be noted that the performance of the numerical simulation could be improved by using other CFD models and comparing the results. Further, if the performance of the main structure of the dam and spillway are considered integrally, it would be more realistic and thus increase the accuracy of the results. Moreover, by developing an agent-based optimization model, the priorities and goals of the stakeholders can be directly included in the optimization process, which significantly increases the compatibility of the designed spillways. In conclusion, the proposed methodology improves the managers' understanding of the effects of flood flow on the design of hydraulic structures and especially stepped spillways and puts a step forward in decision-making processes by incorporating the priorities of stakeholders in finding compromise design scenarios. The selected scenario by this method has a higher executive guarantee and is more compatible with decision-makers' objectives and site-specific conditions.

6. Conclusions

This study proposed a feasible risk-based optimization approach to resolve the conflict in the stepped spillway design. The suggested approach included the FLOW-3D® model and surrogate model (MLP-ANN) to simulate the stepped spillway, CVaR-based NSGA-II for optimization, and the GMCR-plus game model for conflict resolution. Accordingly, the FLOW-3D® model was developed based on laboratory information for two different flow rates over the stepped spillway. Then, the surrogate model was developed using the data from the repeated performance of the numerical simulation. After that, to reach the Pareto optimal solutions, the risk-based optimization model was formed by coupling the MLP-ANN with a novel conditional risk-based NSGA-II algorithm considering conflicting objectives of stakeholders. Lastly, the conflict between stakeholders was resolved by utilizing the GMCR-plus model. The application of the suggested approach in the Jarreh Dam, Iran, resulted in a compromise solution for the stepped spillway design, which simultaneously minimizes the loss in hydraulic performance and the project cost in the form of concrete volume. The paper's main contribution is considering the flood uncertainty and social complexities in the optimal spillway design by a risk-based multi-objective optimization framework and graph model, respectively.

As the directions of future studies, the performance of other numerical models such as FLUENT in 3D simulation of stepped spillways can be compared with the FLOW-3D® model. The data obtained by the MLP model can also be compared with the result of similar existing model to assess their applicability [81]. Moreover, along with hydraulic performance, considering the structural behavior would lead to a comprehensive view of the dam design process and can be pondered as another interesting research line. Furthermore, including the priorities and goals of the stakeholders directly in the optimization process using an agent-based optimization model can considerably elevate the consistency of the optimal spillway design with the real site-specific circumstances.

CRediT authorship contribution statement

Mehrdad Ghorbani Mooselu: Conceptualization, Software, Methodology, Investigation, Writing - original draft, Writing - review & editing, Formal analysis, Visualization. **Mohammad Reza Nikoo:** Conceptualization, Project administration, Supervision, Investigation, Software, Writing - review & editing, Resources. **Parnian Hashempour Bakhtiari:** Conceptualization, Writing - review & editing, Visualization, Software, Formal analysis. **Nooshin Bakhtiari Rayani:** Software. **Azizallah Izady:** Writing - review & editing.

Declaration of competing interest

The authors declare that they have no known competing financial interests or personal relationships that could have appeared to influence the work reported in this paper.

Appendix A. Supplementary data

Supplementary material related to this article can be found online at https://doi.org/10.1016/j.asoc.2021.107721.

References

[1] K.W. Frizell, F.M. Renna, J. Matos, Cavitation potential of flow on stepped spillways, J. Hydraul. Eng. 139 (6) (2012) 630–636.
[2] A. Parsaie, A.H. Haghiabi, M. Saneie, H. Torabi, Prediction of energy dissipation of flow over stepped spillways using data-driven models, Iran. J. Sci. Technol. Trans. Civ. Eng. 42 (1) (2018) 39–53.
[3] M.G. Mooselu, M.R. Nikoo, N.B. Rayani, A. Izady, Fuzzy multi-objective simulation–optimization of stepped spillways considering flood uncertainty, Water Resour. Manag. 33 (7) (2019) 2261–2275.
[4] A. Kuriqi, G. Koçileri, M. Ardiçlioğlu, Potential of Meyer-Peter and Müller approach for estimation of bed-load sediment transport under different hydraulic regimes, Model. Earth Syst. Environ. 6 (1) (2020) 129–137.
[5] A.R.M.T. Islam, S. Talukdar, S. Mahato, S. Kundu, K.U. Eibek, Q.B. Pham, N.T.T. Linh, Flood susceptibility modelling using advanced ensemble machine learning models, Geosci. Front. 12 (3) (2021) 101075.
[6] M.R. Kavianpour, H.R. Masoumi, New approach for estimating of energy dissipation over stepped spillways, Int. J. Civ. Eng. 6 (3) (2008) 230–237.
[7] S.L. Hunt, K.C. Kadavy, The effect of step height on energy dissipation in stepped spillways, in: World Environmental and Water Resources Congress 2009: Great Rivers, 2009, pp. 1–11.
[8] C. Chafi, A. Hazzab, A. Seddini, Study of flow and energy dissipation in stepped spillways, Jordan J. Civ. Eng. 4 (1) (2010) 1–11.
[9] S. Estrella, M. Sánchez-Juny, E. Bladé, J. Dolz, Physical modeling of a stepped spillway without sidewalls, Can. J. Civil Eng. 42 (5) (2015) 311–318.
[10] D.B. Kozlov, I.S. Rumyantsev, Hydraulic studies of stepped spillways of various design, Power Technol. Eng. 49 (5) (2016) 337–344.
[11] C.K. Novakoski, E. Conterato, M. Marques, E.D. Teixeira, G.A. Lima, A. Mees, Macro-turbulent characteristcs of pressures in hydraulic jump formed downstream of a stepped spillway, RBRH (2017) 22.
[12] F.A. Bombardelli, I. Meireles, J. Matos, Laboratory measurements and multi-block numerical simulations of the mean flow and turbulence in the non-aerated skimming flow region of steep stepped spillways, Environ. Fluid Mech. 11 (3) (2011) 263–288.
[13] A. Attarian, K. Hosseini, H. Abdi, M. Hosseini, The effect of the step height on energy dissipation in stepped spillways using numerical simulation, Arab. J. Sci. Eng. 39 (4) (2014) 2587–2594.
[14] H. Shahheydari, E.J. Nodoshan, R. Barati, M.A. Moghadam, Discharge coefficient and energy dissipation over stepped spillway under skimming flow regime, KSCE J. Civ. Eng. 19 (4) (2015) 1174–1182.
[15] A. Bayon, J.P. Toro, F.A. Bombardelli, J. Matos, P.A. López-Jiménez, Influence of VOF technique, turbulence model and discretization scheme on the numerical simulation of the non-aerated, skimming flow in stepped spillways, J. Hydro-Environ. Res. 19 (2018) 137–149.
[16] J.P. Toro, F.A. Bombardelli, J. Paik, I. Meireles, A. Amador, Characterization of turbulence statistics on the non-aerated skimming flow over stepped spillways: a numerical study, Environ. Fluid Mech. 16 (6) (2016) 1195–1221.
[17] F. Salmasi, M. Özger, Neuro-fuzzy approach for estimating energy dissipation in skimming flow over stepped spillways, Arab. J. Sci. Eng. 39 (8) (2014) 6099–6108.
[18] H. Sarkardeh, M. Marosi, R. Roshan, Stepped spillway optimization through numerical and physical modeling, Int. J. Energy Environ. 6 (6) (2015) 597.
[19] M. Bananmah, M.R. Nikoo, B. Nematollahi, M. Sadegh, Optimizing chute-flip bucket system based on surrogate modelling approach, Can. J. Civil Eng. 47 (5) (2020) 584–595.
[20] J.T. Needham, D.W. Watkins Jr, J.R. Lund, S.K. Nanda, Linear programming for flood control in the iowa and des moines rivers, J, Water Resour. Plan. Manag. 126 (3) (2000) 118–127.
[21] C.C. Wei, N.S. Hsu, Optimal tree-based release rules for real-time flood control operations on a multipurpose multireservoir system, J. Hydrol. 365 (3–4) (2009) 213–224.
[22] D.N. Kumar, F. Baliarsingh, K.S. Raju, Optimal reservoir operation for flood control using folded dynamic programming, Water Resour. Manag. 24 (6) (2010) 1045–1064.
[23] D. Karaboga, A. Bagis, T. Haktanir, Controlling spillway gates of dams by using fuzzy logic controller with optimum rule number, Appl. Soft Comput. 8 (1) (2008) 232–238.
[24] N. Asadipoor, V. Mohammad, H. Samani, Spillway gate operation optimization for flood control by means of fuzzy logic, Iran Hydraul. J. 5 (2) (2010) 13–29.
[25] L.G. Shao, X.S. Qin, Y. Xu, A conditional value-at-risk based inexact water allocation model, Water Resour. Manag. 25 (9) (2011) 2125–2145.
[26] M. Soltani, R. Kerachian, M.R. Nikoo, H. Noory, A conditional value at risk-based model for planning agricultural water and return flow allocation in river systems, Water Resour. Manag. 30 (1) (2016) 427–443.
[27] S.S. Naserizade, M.R. Nikoo, H. Montaseri, A risk-based multi-objective model for optimal placement of sensors in water distribution system, J. Hydrol. 557 (2018) 147–159.
[28] M.S. Khorshidi, M.R. Nikoo, M. Sadegh, B. Nematollahi, A multi-objective risk-based game theoretic approach to reservoir operation policy in potential future drought condition, Water Resour. Manag. 33 (6) (2019) 1999–2014.
[29] D.M. Kilgour, K.W. Hipel, The graph model for conflict resolution: Past, present, and future, Group Decis. Negot. 14 (2005) 441–460.
[30] K.D.W. Nandalal, K.W. Hipel, Strategic decision support for resolving conflict over water sharing among countries along the Syr Darya River in the Aral Sea Basin, J. Water Resour. Plan. Manag. 133 (4) (2007) 289–299.
[31] P. Jazayeri, R. Moeini, Optimal design of cascade spillway using meta-heuristic algorithms: comparison of four different algorithms, Environ. Eng. Manag. J. 19 (4) (2020).
[32] S.S. Sammen, M.A. Ghorbani, A. Malik, Y. Tikhamarine, M. AmirRahmani, N. Al-Ansari, K.W. Chau, Enhanced artificial neural network with harris hawks optimization for predicting scour depth downstream of ski-jump spillway, Appl. Sci. 10 (15) (2020) 5160.
[33] Z. Sohrabi, J. Sarvarian, J. Mamizadeh, Development a two-objective simulation-optimization model for optimal design of geometric dimensions and slope of the stepped spillway of upstream siah-bisheh dam using NSGA-II algorithm, Iran. J. Soil Water Res. 51 (2) (2020) 469–478.
[34] K. Hosseini, E.J. Nodoushan, R. Barati, H. Shahheydari, Optimal design of labyrinth spillways using meta-heuristic algorithms, KSCE J. Civ. Eng. 20 (1) (2016) 468–477.
[35] M.K.G. Biglou, A. Pilpayeh, Optimization of Height and Length of Ogee-Crested Spillway by Composing Genetic Algorithm and Regression Models.
[36] A. Ferdowsi, S.F. Mousavi, S. Farzin, H. Karami, Optimization of dam's spillway design under climate change conditions, J. Hydroinform. 22 (4) (2020) 916–936.
[37] M.R. Hassanvand, H. Karami, S.F. Mousavi, Use of multi-criteria decision-making for selecting spillway type and optimizing dimensions by applying the harmony search algorithm: Qeshlagh dam case study, Lakes Reserv.: Res. Manag. 24 (1) (2019) 66–75.
[38] M.M.R. Tabari, M. Hashempour, Development of GWO–DSO and PSO–DSO hybrid models to redesign the optimal dimensions of labyrinth spillway, Soft Comput. 23 (15) (2019) 6391–6406.
[39] O.B. Haddad, M. Mirmomeni, M.A. Marino, Optimal design of stepped spillways using the HBMO algorithm, Civ. Eng. Environ. Syst. 27 (1) (2010) 81–94.
[40] P. Jazayeri, R. Moeini, Construction cost minimisation of the stepped spillway using improved particle swarm optimisation and artificial bee colony algorithms, Water Environ. J. 34 (2020) 468–480.
[41] A. Tavakoli, R. Kerachian, M.R. Nikoo, M. Soltani, S. Malakpour Estalaki, Water and waste load allocation in rivers with emphasis on agricultural return flows: application of fractional factorial analysis, Environ. Monit. Assess. 186 (2014) 5935–5949.
[42] E. Raei, M.R. Alizadeh, M.R. Nikoo, J. Adamowski, Multi-objective decision-making for green infrastructure planning (LID-BMPs) in urban storm water management under uncertainty, J. Hydrol. 579 (2019) 124091.
[43] K. Yenigün, M.U. Ülgen, Trend analysis of maximum flows under climate change evaluation and its impact on spillway safety, Disaster Sci. Eng. 2 (1) (2016) 25–28.
[44] A. Afshar, M.A. Mari no, Optimizing spillway capacity with uncertainty in flood estimator, J. Water Resour. Plan. Manag. 116 (1) (1990) 71–84.
[45] A. Abrishamchi, A. Afshar, R. Kerachian, Spillway capacity optimization under hydrologic uncertainties and flood routing, 2003.
[46] Y. Rahimi, B. Saghafian, M. Banihashemi, Risk-based optimization of flood diversion system of Karun4 dam under hydraulic and hydrologic uncertainties, Iran. J. Soil Water Res. 51 (10) (2020) 2575–2591.
[47] Y.K. Tung, Effects of uncertainties on optimal risk-based design of hydraulic structures, J. Water Resour. Plan. Manag. 113 (5) (1987) 709–722.
[48] Y.K. Tung, L.W. Mays, Optimal risk-based hydraulic design of bridges, J. Water Resour. Plan. Manag. Div. 108 (2) (1982) 191–203.
[49] Y.K. Tung, Y. Bao, On the optimal risk based design of highway drainage structures, Stochast. Hydrol. Hydraul. 4 (4) (1990) 295–308.

[50] A. Afshar, A. Rasekh, M.H. Afshar, Risk-based optimization of large flood-diversion systems using genetic algorithms, Eng. Optim. 41 (3) (2009) 259–273.
[51] A. Rasekh, A. Afshar, M.H. Afshar, Risk-cost optimization of hydraulic structures: methodology and case study, Water Resour. Manag. 24 (11) (2010) 2833–2851.
[52] O.B. Haddad, F. Sharifi, M. Naderi, Optimum design of stepped spillways using genetic algorithm, in: Proceedings of the 6th WSEAS Int. Conf. on Evolutionary Computing, Lisbon, Portugal, pp. 325-331.
[53] K. Roushangar, S. Akhgar, Particle swarm optimization-based LS-SVM for hydraulic performance of stepped spillway, ISH J. Hydraul. Eng. 26 (3) (2020) 273–282.
[54] V.H. Vayghan, A. Saber, S. Mortazavian, Modification of classical horseshoe spillways: Experimental study and design optimization, Civ. Eng. J. 5 (10) (2019) 2093–2109.
[55] S.D. Kim, H.J. Lee, S.D. An, Improvement of hydraulic stability for spillway using CFD model, Int. J. Phys. Sci. 5 (6) (2010) 774–780.
[56] A. Parsaie, A.H. Haghiabi, A. Moradinejad, CFD modeling of flow pattern in spillway's approach channel, Sustain. Water Resour. Manag. 1 (3) (2015) 245–251.
[57] C.W. Hirt, B.D. Nichols, Volume of fluid (VOF) method for the dynamics of free boundaries, J. Comput. Phys. 39 (1) (1981) 201–225.
[58] D.T. Souders, C.W. Hirt, Modeling roughness effects in open channel flows, Flow Sci. (2002).
[59] F.H. Harlow, P.I. Nakayama, Transport of Turbulence Energy Decay Rate (No. la-3854), Los Alamos Scientific Lab. N. Mex, 1968.
[60] V. Yakhot, L.M. Smith, The renormalization group, J. Sci. Comput. 7 (1) (1992) 35–61.
[61] J.W. Deardorff, A numerical study of three-dimensional turbulent channel flow at large Reynolds numbers, J. Fluid Mech. 41 (2) (1970) 453–480.
[62] D.G. Kim, J.H. Park, Analysis of flow structure over ogee-spillway in consideration of scale and roughness effects by using CFD model, KSCE J. Civ. Eng. 9 (2) (2005) 161–169.
[63] X. Cheng, J.S. Gulliver, D. Zhu, Application of displacement height and surface roughness length to determination boundary layer development length over stepped spillway, Water 6 (12) (2014) 3888–3912.
[64] T.S. Bajirao, P. Kumar, M. Kumar, A. Elbeltagi, A. Kuriqi, Superiority of hybrid soft computing models in daily suspended sediment estimation in highly dynamic rivers, Sustainability 13 (2) (2021) 542.
[65] B. Balouchi, M.R. Nikoo, J. Adamowski, Development of expert systems for the prediction of scour depth under live-bed conditions at river confluences: application of different types of ANNs and the M5P model tree, Appl. Soft Comput. 34 (2015) 51–59.
[66] N. Suwal, X. Huang, A. Kuriqi, Y. Chen, K.P. Pandey, K.P. Bhattarai, Optimisation of cascade reservoir operation considering environmental flows for different environmental management classes, Renewable Energy 158 (2020) 453–464.
[67] P. Artzner, F. Delbaen, J.M. Eber, D. Heath, Coherent measures of risk, Math. Finance 9 (3) (1999) 203–228.
[68] R.T. Rockafellar, S. Uryasev, Conditional value-at-risk for general loss distributions, J. Bank. Financ. 26 (7) (2002) 1443–1471.
[69] R.T. Rockafellar, S. Uryasev, Optimization of conditional value-at-risk, J. Risk 2 (2000) 21–42.
[70] E. Zitzler, Evolutionary Algorithms for Multi-Objective Optimization: Methods and Applications, Vol. 63, Ithaca, Shaker, 1999.
[71] N. Riquelme, C. Von Lücken, B. Baran, Performance metrics in multi-objective optimization, in: 2015 Latin American Computing Conference (CLEI), IEEE, 2015, pp. 1–11.
[72] C. Audet, J. Bigeon, D. Cartier, S. Le Digabel, L. Salomon, Performance indicators in multi-objective optimization, European J. Oper. Res. (2020).
[73] T. Okabe, Y. Jin, B. Sendhoff, A critical survey of performance indices for multi-objective optimisation, in: The 2003 Congress on Evolutionary Computation, 2003. CEC'03, Vol. 2, IEEE., 2003, pp. 878–885.
[74] R.A. Kinsara, O. Petersons, K.W. Hipel, D.M. Kilgour, Advanced decision support for the graph model for conflict resolution, J. Decision Syst. 24 (2) (2015) 117–145.
[75] J.F. Nash, Equilibrium points in n-person games, Proc. Natl. Acad. Sci. 36 (1) (1950) 48–49.
[76] N. Howard, Paradoxes of Rationality: Theory of Metagames and Political Behavior, Vol. 1, MIT press, 1971.
[77] K.W. Hipel, D.M. Kilgour, L. Fang, X.J. Peng, The decision support system GMCR in environmental conflict management, Appl. Math. Comput. 83 (2–3) (1997) 117–152.
[78] N. Taravatrooy, M.R. Nikoo, J.F. Adamowski, N. Khoramshokooh, Fuzzy-based conflict resolution management of groundwater in-situ bioremediation under hydrogeological uncertainty, J. Hydrol. 571 (2019) 376–389.
[79] W. Wan, B. Liu, A. Raza, Numerical prediction and risk analysis of hydraulic cavitation damage in a high-speed-flow spillway, Shock Vib. (2018).
[80] J. Zeng, Z. Rakib, M. Ansar, S. Hajimirzaie, Optimization and risk assessment in design and operation of hydraulic structures using three-dimensional CFD modeling, in: World Environmental and Water Resources Congress 2020: Hydraulics, Waterways, and Water Distribution Systems Analysis, American Society of Civil Engineers, Reston, VA, 2020, pp. 170–182.
[81] N. Taravatrooy, F. Bahmanpouri, M.R. Nikoo, C. Gualtieri, A. Izady, Estimation of air-flow parameters and turbulent intensity in hydraulic jump on rough bed using Bayesian model averaging, Appl. Soft Comput. 103 (2021) 107165.